Two-Transmitter Wireless Power Transfer with Optimal Activation and Current Selection of Transmitters

Sungryul Huh and Dukju Ahn

***Abstract*—The paper proposes optimal driving conditions of two transmitters (TXs) in magnetic wireless power transfer, where the couplings from each TX to an RX are not identical. First, for the case of identical TX coil currents, a criterion for deactivating a specific TX element is proposed. Specifically, one TX element among the two TXs often has weaker coupling coefficient than the other TX element. It is found that the TX element with weaker coupling should be deactivated if its coupling coefficient is less than 0.414 times of the stronger coupling. Second, for the case of adjustable TX coil currents, the optimal current ratio between the two TX coils is proposed. It is found that the TX coil current ratio should be equal to the coupling coefficient ratio, e.g., the TX coil with twice coupling with an RX should carry twice current. The results are widely applicable regardless of absolute coupling strength and load condition because it turns out that the results only depend on the ratio of couplings. Finally, it is discussed that the required component values of an LCC inverter should be adjusted based on the current ratios and coupling between adjacent TXs.**

***Index Terms*—Inductive wireless power transfer, LCC resonant inverter, multiple transmitters, two transmitters.**

I. Introduction

THE need for the arrayed transmitter (TX), where multiple small transmitters are laid out to accommodate wider charging space, is increasing in inductive wireless power transfer system. An application is wireless charging pad that consists of two TX coils to cover wide area and lateral misalignments. For example, transmitter designs A4, A14, or A19 of [28] are the arrayed TX that contains two TX coils within a TX device.

There are several literature that address the wide charging surface. The works [1]–[3] propose novel winding methods which can create uniform magnetic field across the transmitter surface. However, since the receiver is located only in narrow portion of wide surface, it would be inefficient to generate the magnetic field across the entire area. The works [4]–[6] utilize segmented TX coil elements. Especially, [4] equips with small TX coils which are parallel-connected to the common driving source. The drawback of the scheme is that all four TX coils are activated regardless of the position of receiver. This leads to the power dissipation due to the conduction loss of circulating current at all four TX locations. It would be more efficient to deactivate a specific TX element if the element is very weakly coupled with the receiver. The same problem may arise in [6].

The works [7]–[9] propose selective activation of a TX element among the many elements of TX array. The efficiency is improved by selectively activating a (set of) TX element depending on the receiver location. In [7], the outer diameter of coils is specially designed such that at least one TX coil is contained within receiver. In [7, Fig. 10], three TX coils are able to deliver power to the receiver. However, only one TX is selected at a time in [7].

There is room to improve the efficiency further if multiple transmitters can simultaneously operate for one receiver. The work [10] demonstrated that a simultaneous 2-TX operation achieves higher efficiency than 1-TX. On the other hand, a conflicting result has been drawn from [11] where the respective distances between each TX to an RX are swept. Referring to [11, Fig. 1], 1-TX system shows higher efficiency than 2-TX system if the receiver is placed closer to a specific TX than other TX. The work [12] discusses that the 2-TX system achieves higher efficiency if the respective couplings between each TX and an RX are the same, and that the 2-TX may become inferior if one TX is weakly coupled to an RX compared to the other TX. Summarizing the results in [10]–[12], the 2-TX system may or may not achieve higher efficiency depending on the receiver location relative to each transmitter. However, so far, exact theoretical criterion has not yet been reported regarding the boundary condition at which 2-TX (or 1-TX) starts to outperform the 1-TX (or 2-TX) system.

Another limitation of aforementioned prior works is that the input voltage sources for the 2-TX are assumed to be identical. There are some works which adjust the TX coil currents. The work [13] proposes a method to focus the magnetic field on a specific location by adjusting the strength and sign of coil current. As a result, very sharp magnetic field shape can be obtained with high spatial resolution. This is useful to avoid harmful electromagnetic interference and electromotive force effects to surrounding areas while successfully delivering the power to the desired location. However, the efficiency aspect of the system is not yet evaluated. The work [14] successfully maximizes the efficiency of 2-TX system by adjusting the voltage

Manuscript received February 12, 2017; revised April 5, 2017 and May 26, 2017; accepted July 4, 2017. Date of publication July 11, 2017; date of current version February 22, 2018. This work was supported by the National Research Foundation (2016R1D1A1B03930682). Recommended for publication by Associate Editor Chun T. Rim. *(Corresponding author: Dukju Ahn.)*

The authors are with Incheon National University, Incheon 22012, South Korea (e-mail: tjdfuf2397@naver.com; dahn@inu.ac.kr).

Color versions of one or more of the figures in this paper are available online at http://ieeexplore.ieee.org.

Digital Object Identifier 10.1109/TPEL.2017.2725281

sources which model a voltage mode inverter. As will be discussed in Section III, a formula in terms of TX coil current can be more generally applicable than the formula in voltage source.

This paper investigates theoretical aspects of optimal driving of 2-TX system where the respective couplings from each TX to an RX are different. The first case is with identical current for the 2-TX coils. In simple and low-cost applications, the TX coil currents in the TX array are often fixed to be identical. To maximize the efficiency of total system, the criterion for selecting between 1-TX and 2-TX operation is studied. The result is that the TX element, which is weakly coupled with the RX than the other TX element, should be deactivated if the weak coupling is lower than 0.414 times of the stronger coupling. If the weaker coupling is higher than 0.414 times of stronger coupling, then the simultaneous 2-TX operation is better.

The second case is for more complex applications where it is possible to adjust each TX current in TX array. It is found that the TX coil currents should be scaled proportional to the ratio of coupling coefficients. In other words, different TXs have different couplings with an RX, and each TX coil current should be proportional to their respective coupling with an RX.

Also discussed is the practical inverter consideration for 2-TX operation. The two TX coils are typically placed such that significant portion of one TX is overlapped with adjacent TX in order to remove null point and provide uniform coverage [15], [16]. The overlap between adjacent TX causes magnetic coupling, which should be considered in practical inverter implementation. The variation of effective inductance of TX coil due to the variations of adjacent TX current is formulated, and this is used to maintain soft-switching of inverter switches.

Interestingly, the above-mentioned results are independent of receiver load, absolute strength of coupling, and parasitic resistance, as long as the two TXs have identical coil inductances and parasitics. This is usually the case in arrayed-type multiple TXs. Another key benefit over previous works is that the analytical results are formulated in terms of TX coil currents and, therefore, can be generally applied to wide variety of TX inverter topologies regardless of inverter compensation and resonance tuning. In other words, there are many different types of inverters whose voltage to coil-current relation is totally different. Moreover, even a given topology of an inverter can exhibit completely different voltage to coil-current relation. Therefore, formulation in terms of coil current can be more easily used than that in terms of input voltage.

Section II discusses the 2-TX system with the TX coil currents being fixed to be identical to each other. Section III analyzes the case where the respective coil currents of two TXs are allowed to be adjustable. Section IV discusses the variation of effective inductance of coils and its impact on multiple-TX inverter design. Section V presents measurement results. Section VI draws conclusions.

II. Criteria for Selecting Transmitter Combination

Referring to Fig. 1, the system efficiency is the received power divided by the total power dissipation in the system, which can

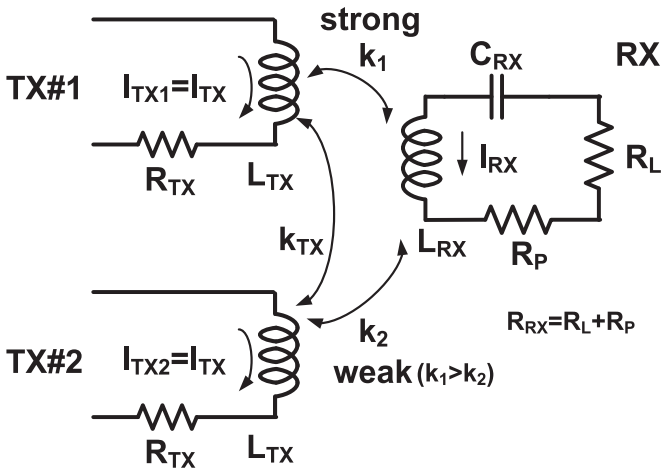

Fig. 1. Two identical TX coils have the same current $I_{\rm TX}$ and component values. The receiver is closer to TX#1 than TX#2, and therefore $k_1 > k_2$.

be written as

$$\begin{aligned}\text{eff} &= \frac{|\mathbf{I_{RX}}|^2 R_{\rm RX}}{R_{\rm TX}|\mathbf{I_{TX1}}|^2 + R_{\rm TX}|\mathbf{I_{TX2}}|^2 + |\mathbf{I_{RX}}|^2 R_{\rm RX}} \frac{R_L}{R_{\rm RX}} \\ &= \frac{|\mathbf{I_{RX}}|^2 R_{\rm RX}}{2R_{\rm TX}|\mathbf{I_{TX}}|^2 + |\mathbf{I_{RX}}|^2 R_{\rm RX}} \frac{R_L}{R_{\rm RX}} \\ &= \frac{R_{\rm RX}}{2R_{\rm TX}\left|\frac{\mathbf{I_{TX}}}{\mathbf{I_{RX}}}\right|^2 + R_{\rm RX}} \frac{R_L}{R_{\rm RX}} \end{aligned} \tag{1}$$

where the two transmitters are assumed to be identical which is typically the case in simple transmitter array. The case of different TX currents will be analyzed in next section. To obtain the analytical expression of $\mathbf{I_{TX}}/\mathbf{I_{RX}}$ for Fig. 1, a Kirchhoff's voltage law (KVL) equation for receiver coil path is used at the resonant frequency of RX as follows:

$$\begin{aligned} j\omega k_1\sqrt{L_{\rm TX}L_{\rm RX}}\mathbf{I_{TX}} + j\omega k_2\sqrt{L_{\rm TX}L_{\rm RX}}\mathbf{I_{TX}} \\ + R_{\rm RX}\mathbf{I_{RX}} = 0. \end{aligned} \tag{2}$$

Although the coupling between TXs, $k_{\rm TX}$, is considered in Fig. 1, the term $k_{\rm TX}$ does not appear in (1) and (2). Equation (1) depends only on the currents and resistances because the inductive impedance does not dissipate power. The coupling between TXs changes the effective inductance seen by inverters as in Section IV. However, inductive impedances do not dissipate power. Therefore, it does not affect the efficiency definition (1). Next, (2) is the voltages across the receiver loop. The RX voltage depends on mutual inductance between $L_{\rm TX} - L_{\rm RX}$ and TX coil current as in (9). The $k_{\rm TX}$ does not appear at (2). Rather, $k_{\rm TX}$ may change the tuning capacitor or input voltage that is required to produce the specified TX coil current $\mathbf{I_{TX}}$ (discussed in Section IV). However, even if the tuning capacitor or input voltage required to produce the specified $\boldsymbol{I}_{TX}$ is changed, they do not affect the equation because the voltage induced on RX depends only on $\boldsymbol{I}_{TX}$ and $L_{\rm TX} - L_{\rm RX}$ *by the definition of mutual inductance*. The fundamental definition of

mutual inductance is $v_{\mathrm{RX}} = M_{\mathrm{TX-RX}} \frac{di_{\mathrm{TX}}}{dt}$, which states that the RX voltage depends only on TX–RX coupling and TX coil current, not on the capacitors or input voltage. In other words, although k_{TX} may affect the capacitors or input voltage (depending on inverter topology), the RX voltage is on the direct form of $\boldsymbol{I}_{TX}$, and the term k_{TX} does not directly appear when writing (2).

The currents ($\boldsymbol{I}_{TX}$) induced by two different TXs can be in-phase if 1) they are driven by a common clock signal and 2) some inverters (e.g., LCC, push–pull current-fed, current-feedback) enforce the magnitude and phase of $\boldsymbol{I}_{TX}$ currents to be the same. For the case of the LCC inverter, $\boldsymbol{I}_{TX}$ by the LCC inverter is dependent only on C_P and V_{d} of Fig. 5. This has been discussed in [19, (3)–(7)], i.e., $\mathbf{I_{TX}} = -j\omega C_P \mathbf{V_d}$. Therefore, the $\boldsymbol{I}_{TX}$ of the two inverters can be the same because $\boldsymbol{V}_d$, C_P, and ω are the same. Pantic *et al.* [19], [22] state that the coil current is load independent. Appendix B shows the derivations. For a push–pull current-fed inverter [20], the TX coil current is also insensitive to coupling. Even a simple series-resonant inverter can produce constant TX coil current by current sensing and feedback control [22].

The current ratio $\mathbf{I_{TX}}/\mathbf{I_{RX}}$ is found directly from (2)

$$\frac{\mathbf{I_{TX}}}{\mathbf{I_{RX}}} = -\frac{1}{jQ_{\mathrm{RX}}} \frac{1}{k_1 + k_2} \sqrt{\frac{L_{\mathrm{RX}}}{L_{\mathrm{TX}}}} \tag{3}$$

where $Q_{\mathrm{RX}} = \omega L_{\mathrm{RX}}/R_{\mathrm{RX}}$.

We would like to compare the two-transmitter system and the one-transmitter system in terms of overall system efficiency. The efficiency of 1-TX system is written as

$$\begin{aligned} \mathrm{eff}_{1\mathrm{TX}} &= \frac{|\mathbf{I_{RX-1TX}}|^2 R_{\mathrm{RX}}}{R_{\mathrm{TX}}|\mathbf{I_{TX-1TX}}|^2 + |\mathbf{I_{RX-1TX}}|^2 R_{\mathrm{RX}}} \frac{R_L}{R_{\mathrm{RX}}} \\ &= \frac{R_{\mathrm{RX}}}{R_{\mathrm{TX}} \left| \frac{\mathbf{I_{TX-1TX}}}{\mathbf{I_{RX-1TX}}} \right|^2 + R_{\mathrm{RX}}} \frac{R_L}{R_{\mathrm{RX}}} \end{aligned} \tag{4}$$

where its current ratio is

$$\frac{\mathbf{I_{TX-1TX}}}{\mathbf{I_{RX-1TX}}} = -\frac{1}{jQ_{\mathrm{RX}}} \frac{1}{k_1} \sqrt{\frac{L_{\mathrm{RX}}}{L_{\mathrm{TX}}}}. \tag{5}$$

Having found the efficiency expressions for the cases of 1-TX and 2-TX, a key question is which transmitter configuration can achieve higher efficiency. To solve the problem, a condition will be investigated such that the 2-TX efficiency (1) is higher than the 1-TX efficiency (4) as follows:

$$\frac{R_{\mathrm{RX}}}{2R_{\mathrm{TX}} \left| \frac{\mathbf{I_{TX}}}{\mathbf{I_{RX}}} \right|^2 + R_{\mathrm{RX}}} \geq \frac{R_{\mathrm{RX}}}{R_{\mathrm{TX}} \left| \frac{\mathbf{I_{TX-1TX}}}{\mathbf{I_{RX-1TX}}} \right|^2 + R_{\mathrm{RX}}}. \tag{6}$$

To satisfy the inequality

$$2\left| \frac{\mathbf{I_{TX}}}{\mathbf{I_{RX}}} \right|^2 \leq \left| \frac{\mathbf{I_{TX-1TX}}}{\mathbf{I_{RX-1TX}}} \right|^2 \quad \text{or} \quad \frac{2}{(k_1 + k_2)^2} \leq \frac{1}{k_1^2}. \tag{7}$$

Rearranging the condition (7) yields

$$k_2 \geq \left(\sqrt{2} - 1\right) k_1 \approx 0.41 k_1. \tag{8}$$

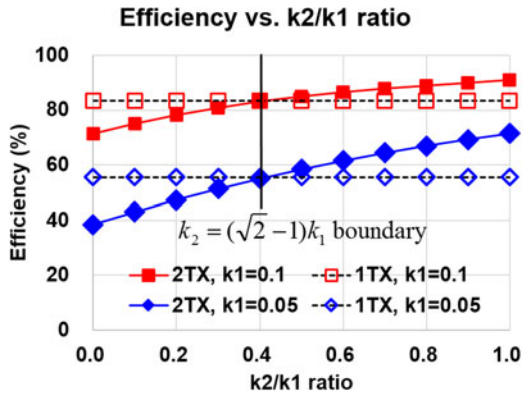

Fig. 2. Efficiency versus k_2/k_1 ratio for Fig. 1. For red square traces, k_1 is set to 0.1. For blue diamond traces, $k_1 = 0.05$. For all cases, the weakly coupled TX (TX#2) should be turned-OFF if the weak coupling (k_2) is below 0.41 times of stronger coupling (k_1). $R_{\mathrm{TX}} = 0.25$, $R_{\mathrm{RX}} = 5$. $L_{\mathrm{TX}} = L_{\mathrm{RX}} = 20\,\mu$H. $f = 200$ kHz.

Expression (8) indicates that the efficiency of 2-TX system is higher than 1-TX when the weaker coupling (k_2) is higher than 0.41 times of the stronger coupling (k_1). Another statement is that the TX with lower coupling should be turned-OFF if its coupling with RX is lower than 0.41 times of stronger coupling.

Note that the condition specifies *only the relative ratio of two coupling coefficients* k_1 and k_2. The load resistance R_L, the absolute strength of k_1 and k_2, the intracoupling between the two TXs, and the parasitic resistance of coils do not affect (8).

It is reported for the first time in this paper that only the relative ratio of coupling serves as the criterion for the number of activated TX. Some previous literature have discussed the advantage of having two transmitters to power one receiver [12]. However, the boundary criterion, below which the 2-TX system becomes inferior to the single-TX system, has not been analyzed elsewhere. Qualitatively, it is natural to deactivate a transmitter which is very weakly coupled to the receiver. Equation (8) clarifies the exact boundary below which the weakly coupled transmitter should be deactivated for high efficiency.

Fig. 2 presents simulated efficiencies for various coupling configurations. For red square traces, k_1 is fixed to 0.1 and k_2 is swept from 0 to 0.1. For blue diamond traces, k_1 is fixed to 0.05 and k_2 is swept across 0–0.05. For 1-TX systems, only k_1 is activated and k_2 is OFF. It can be seen that the 2-TX systems perform better when $k_2 > 0.4k_1$. However, for the region of $k_2 < 0.4k_1$, the 2-TX systems become inefficient and the weakly coupled TX should be therefore turned OFF.

One more note is that the derivations (1)–(8) are valid for the *same coil currents for the two transmitters*. In some cases where the simple series-tuned resonant inverter is used, the two coil currents which are the output current of each inverter become different depending on the relative ratio of k_1 and k_2. For example, Ahn and Hong [12] consider two voltage-source inverters, where the asymmetry between k_1 and k_2 indeed changes the TX coil currents, resulting in different TX coil currents from each other. Therefore, the basic assumption of [12] and the result are different from this paper. Ahn and Hong [12] claim that the

required k_2/k_1 ratio is varied depending on the strength of k_2 and k_1. This is the case when the simple fully compensated voltage-source inverter is used, where the coil current is unpredictable depending on coupling, load, and inverter parameters. On the other hand, many practical systems maintain constant TX coil currents in response to coupling and load variations for stable operation [17], [22]. Equation (8) is universally applicable in this case. There are inverter topologies which produce constant coil current such as LCC [17]–[19] or push–pull parallel-resonant inverter [20], [21].

III. Two Transmitters With Adjustable Current

In some system where complex control circuitry is allowed, the coil currents of the two transmitters can be adjusted to be different from each other. There exists a set of TX parameters that maximize the overall efficiency. For example, in [14] the input source voltages are optimized for maximum efficiency. Ideal voltage source which resembles fully compensated series-resonant inverter is assumed. However, practical series-resonant inverter is designed to drive inductive load for high efficiency. The voltage source behavior of fully compensated series-resonant inverter makes the current and voltage unstable in response to coupling or load variations [22].

In general, by the definition of mutual inductance, the voltage induced at secondary coil is written as

$$v_2 = M\frac{di_1}{dt} = k\sqrt{L_1 L_2}\frac{di_1}{dt} \tag{9}$$

which indicates that the only transmitter parameter that affects the received voltage is the TX coil current [i_1 in (9)] and TX inductance. In other words, the TX input voltage or TX tuning capacitor does not directly affect the received voltage. Instead, source voltage might alter the TX coil current and thus indirectly affects the received voltage. The relation between source voltage and TX coil current depends on many factors including compensation topology, TX resonance frequency, coupling, and receiver load. Therefore, the characterization using source voltage is not universally applicable to various compensation topology and TX resonance tuning.

Therefore, in this paper, coil currents condition is investigated to obtain a generally applicable formula instead of voltage source condition. Referring to Fig. 3, denote coil currents at TX#1 and TX#2 as $\boldsymbol{I}_{TX}$ and $A\boldsymbol{I}_{TX}$, respectively, where A is a scaling factor and can be either larger or smaller than unity during derivation procedure.

The efficiency with two different TX currents is written as

$$\begin{aligned}\text{eff} &= \frac{|\mathbf{I_{RX}}|^2 R_{\text{RX}}}{R_{\text{TX}}|\mathbf{I_{TX}}|^2 + R_{\text{TX}}|A\mathbf{I_{TX}}|^2 + |\mathbf{I_{RX}}|^2 R_{\text{RX}}}\frac{R_L}{R_{\text{RX}}} \\ &= \frac{R_{\text{RX}}}{R_{\text{TX}}\left|\frac{\mathbf{I_{TX}}}{\mathbf{I_{RX}}}\right|^2 (1+A^2) + R_{\text{RX}}}\frac{R_L}{R_{\text{RX}}}.\end{aligned} \tag{10}$$

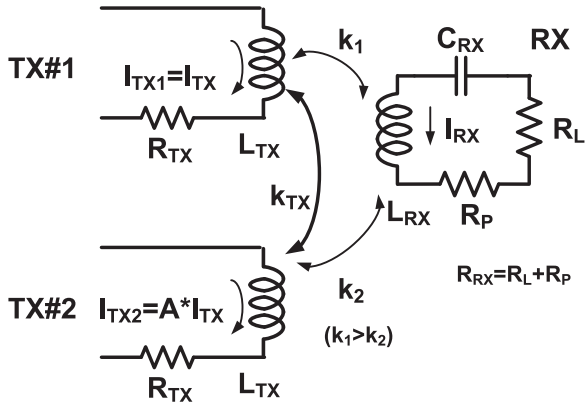

Fig. 3. Similar to Fig. 1 except that the TX coil currents are allowed to be different. The currents at TX#1 and TX#2 are $\mathbf{I_{TX}}$ and $A_*\mathbf{I_{TX}}$, respectively, where A is an arbitrary scaling factor which can be higher or lower than unity.

The current ratio $\mathbf{I_{TX}}/\mathbf{I_{RX}}$ is found by KVL equation on RX current loop

$$\begin{aligned}j\omega k_1\sqrt{L_{\text{TX}}L_{\text{RX}}}\mathbf{I_{TX}} + j\omega k_2\sqrt{L_{\text{TX}}L_{\text{RX}}}A\mathbf{I_{TX}} \\ + R_{\text{RX}}\mathbf{I_{RX}} = 0\end{aligned} \tag{11}$$

which gives the current ratio

$$\frac{\mathbf{I_{TX}}}{\mathbf{I_{RX}}} = -\frac{1}{jQ_{\text{RX}}}\frac{1}{k_1 + Ak_2}\sqrt{\frac{L_{\text{RX}}}{L_{\text{TX}}}}. \tag{12}$$

To maximize the efficiency in (10), the following expression is differentiated with respect to the scaling factor A:

$$\frac{d}{dA}\frac{1+A^2}{(k_1 + Ak_2)^2} = 0. \tag{13}$$

The final result is

$$A = \frac{k_2}{k_1} \tag{14}$$

which states that the current at TX#2 should be scaled according to the ratio of coupling coefficient. For example, if the coupling between TX#2 and RX is half of the coupling between TX#1 and RX, then the coil current at TX#2 should be scaled to half.

Note that the result (14) also does not depend on the RX load, the absolute strength of coupling, the parasitic resistance of coils, and the intracoupling between adjacent TXs. It is the relative ratio of two couplings that determines the required TX coil current ratio for the highest efficiency.

Fig. 4 presents the efficiencies for various TX coil current ratios. The red circle trace is for the k_2/k_1 ratio of 0.8. Its maximum efficiency occurs when the TX coil current ratio $A = I_{\text{TX}2}/I_{\text{TX}1}$ is equal to coupling ratio 0.8. The black triangle trace is for the k_2/k_1 ratio of 0.4, and the maximum efficiency occurs at the TX current ratio of 0.4.

IV. Inverter Coupling Consideration for Multiple TXs

The LCC resonant inverter of Fig. 5 is chosen rather than the simple series-resonant inverter due to the stability in TX coil current. The magnitude and phase of coil current of the LCC

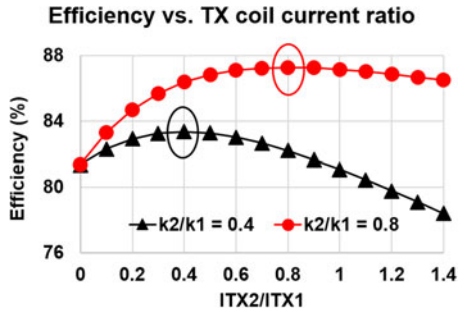

Fig. 4. Efficiency versus TX current ratio for Fig. 3. For black triangle trace, the ratio of k_2/k_1 is 0.4. For red circle trace, the ratio of k_2/k_1 is 0.8. The maximum efficiencies occur when the TX coil current ratio $A = I_{\mathrm{TX2}}/I_{\mathrm{TX1}}$ is equal to the coupling ratio. $L_{\mathrm{TX}} = 14.6\,\mu$H. $L_{\mathrm{RX}} = 13.9\,\mu$H. $R_{\mathrm{TX}} = R_P = 0.15$. $R_L = 10$.

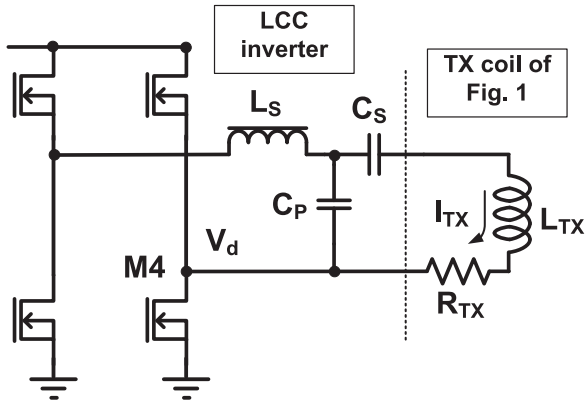

Fig. 5. Notations and topology of the LCC resonant inverter in this paper.

inverter is constant regardless of the coupling or load changes as discussed in [19], which is desired for stable operation. The TX coil current is proportional to the inverter input voltage regardless of coupling or load conditions. Therefore, it is easy to set the current ratio between TX coils as required by previous sections.

When the two TX coils form a TX array, the two TX coils are laid out to have geometrical overlap with each other to remove null points [15], [16]. This overlap causes intracoupling between TX coils within a TX array. It has been discussed in [12] that the TX resonance frequency is altered due to the intracoupling. However, the general case of different coil currents and its impact on inverter are not analyzed elsewhere.

The coupling between the two TX coils modifies the effective inductance of the TX coils. Then, the component values of other passive components in inverter need to be modified considering the coupling between TXs. It is important to estimate the effective inductance due to the coupling under the array condition.

Referring to Fig. 6, the two TX coils carry different magnitude of currents as in the case of previous sections. The KVL equation for the TX#1 coil is

$$\mathbf{V_{COIL1}} = j\omega L_{\mathrm{TX}}\mathbf{I_{TX1}} + j\omega k_{\mathrm{TX}}\sqrt{L_{\mathrm{TX}}L_{\mathrm{TX}}}\mathbf{I_{TX2}}. \quad (15)$$

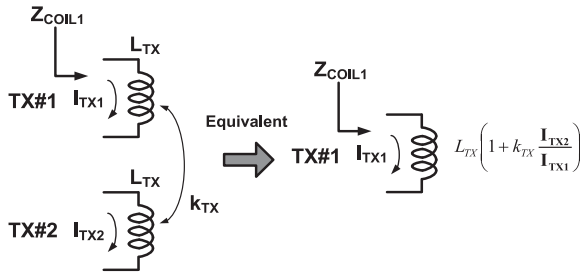

Fig. 6. Two adjacent TX coils are coupled to each other by a coupling coefficient k_{TX}. Denote the currents at TX#1 and TX#2 as I_{TX1} and I_{TX2}, respectively. The effective coil inductance of TX#1 is increased as in the right side of equivalent circuit.

The impedance of TX#1 coil is found using (15) as

$$\mathbf{Z_{COIL1}} = \frac{\mathbf{V_{COIL1}}}{\mathbf{I_{TX1}}} = j\omega L_{\mathrm{TX}} + j\omega L_{\mathrm{TX}} k_{\mathrm{TX}} \frac{\mathbf{I_{TX2}}}{\mathbf{I_{TX1}}}$$
$$= j\omega L_{\mathrm{TX}} \left(1 + k_{\mathrm{TX}} \frac{\mathbf{I_{TX2}}}{\mathbf{I_{TX1}}}\right) \quad (16)$$

which states that the coil impedance is initially $j\omega L_{\mathrm{TX}}$ but increased by a factor of $k_{\mathrm{TX}}\mathbf{I_{TX2}}/\mathbf{I_{TX1}}$ when adjacent coil is activated.

Although the output coil current of the LCC inverter is constant regardless of such variation of inductance, the efficiency of inverter may degrade significantly if proper adjustments of component values are not performed against such inductance variation.

The nominal design equations of the LCC inverter of Fig. 5 are

$$\frac{1}{\sqrt{L_S C_P}} = \omega \quad (17\text{-a})$$

$$\frac{1}{\sqrt{(L_{\mathrm{TX}} - L_S)C_S}} = \omega. \quad (17\text{-b})$$

Fig. 7(a) presents normal waveforms with single TX operation. The switch current $i_{,M4}$ is small and the switch is turned ON at low V_d voltage, leading to low switching loss. On the other hand, Fig. 7(b) presents waveforms when the adjacent TX is coupled to this TX and is activated with the same magnitude of current. This case is equivalent to the L_{TX} increment by a factor of $1 + k_{\mathrm{TX}}$. The switch current $i_{,M4}$ shows spike at turn ON instance of switch, 241.7 μs, which means the failure of soft-switching and high switching loss. Also note that the switch current $i_{,M4}$ and the inductor current $i_{,\mathrm{LS}}$ are higher than Fig. 7(a) while producing the same coil current $\boldsymbol{I}_{TX}$. This leads to higher conduction loss than the case of Fig. 7(a). Moreover, not only the coupling itself but also the current ratio between adjacent TX and this TX affects the effective inductance and component adjustment. L_{TX} is 14.6 μH, k_{TX} is 0.117, $L_S = 2.5\,\mu$H, $C_S = 23.3$ nF, and $C_{\mathrm{p}} = 114$ nF.

Therefore, the tuning capacitor C_{S} of the LCC inverter needs to be adjusted for each ratio of TX coil currents such that (17-b) is still satisfied with the modified L_{TX} value. In the experiments in this paper, the tuning capacitor C_{S} is manually adjusted for each different current ratio. In actual automated system, relay

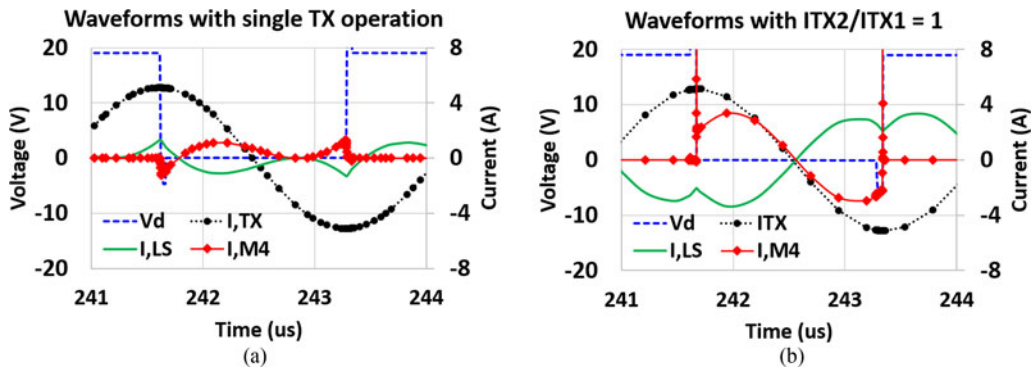

Fig. 7. Waveforms of the LCC inverter. (a) Normal single-TX condition. (b) Adjacent TX starts operating. Deviations in inductance values. The currents on MOSFET switches and compensation inductor are significantly increased, leading to higher losses.

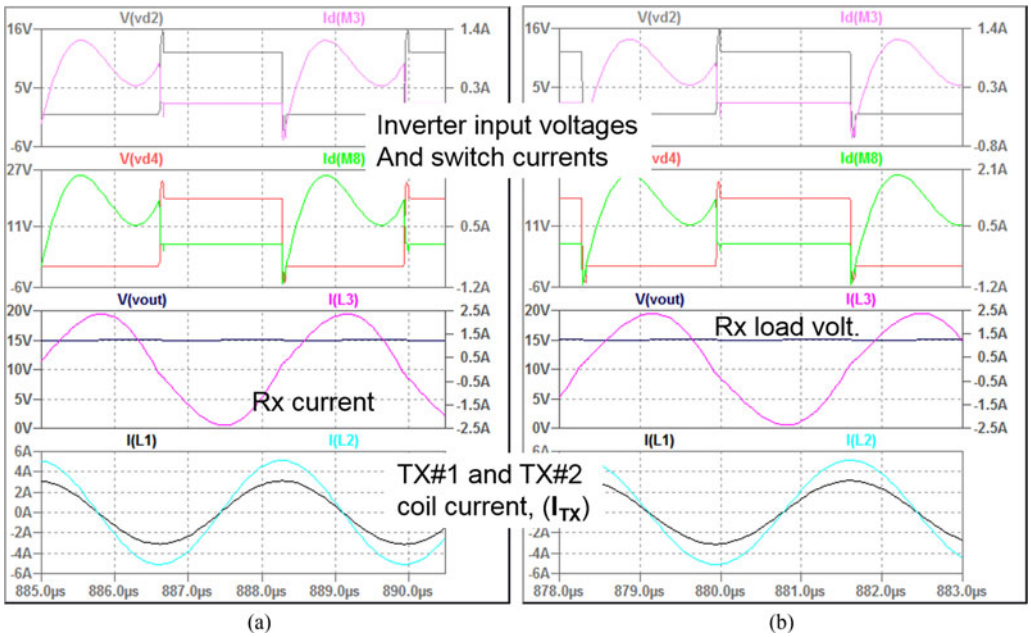

Fig. 8. Simulation with and without the intra coupling k_{TX}. For the k_1/k_2 ratio of 0.6. The $\mathbf{I_{TX1}/I_{TX2}}$ is therefore set to 0.6 as in (14). The overall system efficiency with and without k_{TX} is simulated as 83.0% for both cases. (a) Without coupling between TXs. $L_{\mathrm{TX}} = 14.6\,\mu$H and $C_S = 23.26$ nF for TX#1 and TX#2. (b) With coupling of 0.1 between TXs. C_S of TX#1 and TX#2 are 19.4 and 21.7 nF, respectively.

switches [24] or dynamic resonance tuning [23] would be necessary to reconfigure C_S for each TX current ratio.

Although the intracoupling k_{TX} changes the effective impedance seen by the inverter and consequently the tuning capacitor C_S, it does not affect the efficiency or output power level as long as correct tuning capacitor is selected. Fig. 8 shows the simulation results with and without k_{TX}. The resultant TX coil current $\boldsymbol{I}_{TX}$, the RX current and load voltage, and inverter switch currents are the same for both cases regardless of coupling between TXs. The total efficiency is also simulated to be identical. This is possible because the tuning capacitor C_S is designed to be different accounting for k_{TX}.

V. Experiment Results and Discussion

Fig. 9 shows experiment setup. In TX arrays, the adjacent transmitter coils should be close together and should have an overlap in order to remove the "dead zone" between transmitters. The necessity of overlap between adjacent TXs has been discussed in [29] and [30]. Each TX coil is fed by its dedicated LCC resonant inverter. A board on the left-side of Fig. 9(a) contains two independent LCC inverters with separated dc inputs and ac outputs, except that the gate drive signals share a common clock. For 2-TX case, it is possible for the one PCB to contain two inverters. However, for larger number of array, the inverters would use separate PCBs. In this case, the clocks can be shared by signaling wires. In fact, to operate separate inverter PCBs, wire connections between inverters and a master controller are necessary because each inverter PCB requires a dc power input and control signals as well as the clocks from an external controller. Such example can be found in [16].

The RX coil is connected to rectifier board on right-side of Fig. 9(a). The vertical distance between TX plane and RX plane is varied across 2.5–5.8 cm, although the photos are taken from top view and vertical separation is therefore not visible. Electronic load equipment serves as a load for the RX. The

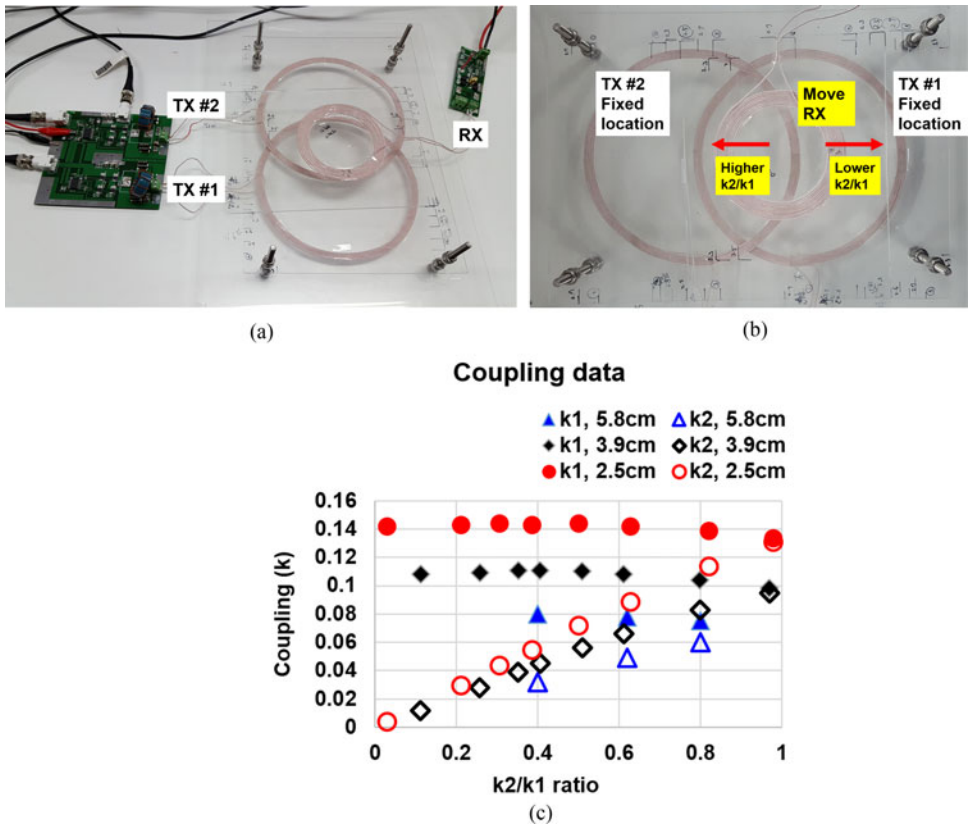

Fig. 9. (a) Overall experiment setup. (b) The RX location is for $k_1/k_2 = 0.6$. Moving the RX toward left for a given vertical separation leads to higher k_2/k_1 ratio. (c) Coupling coefficients for various vertical separations between TX and RX throughout the experiments.

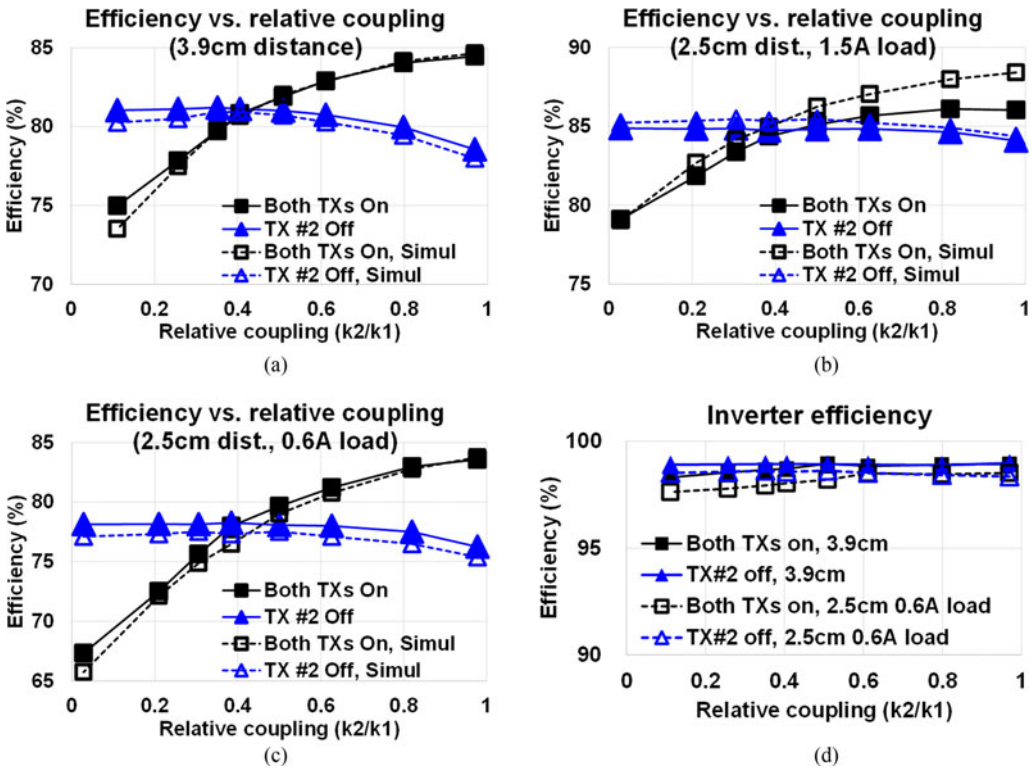

Fig. 10. Comparison between 2-TX and 1-TX operation. 2-TX operation is more efficient if the weaker coupling (k_2) is higher than 0.41 times of stronger coupling (k_1). (a) Vertical separation between TX and RX is 3.9 cm. (b) Vertical separation of 2.5 cm. (c) 2.5 cm separation with reduced load current. (d) Simulated inverter efficiencies for (a) and (c). The inverter efficiency is relatively constant compared to the large variations of overall efficiencies of (a)–(c).

operating frequency is 300 kHz. The diameter of TX and RX coils is 17 and 9.5 cm, respectively. The number of turns for TX and RX coils are 6 and 10, respectively. The inductance of TX coil and RX coil are 14.6 and 13.9 μH, respectively. The measured parasitic resistance of coils is 0.15 and 0.14 Ω for TX and RX coils, respectively. The Q-factors of TX and RX coil are 183 and 187, respectively. The coil is fabricated using 0.06 mm 200 strands Litz wire. The intracoupling between two TXs, k_{TX}, is measured to be 0.117.

Fig. 9(b) shows the RX location when $k_2/k_1 = 0.61$. For given vertical separation, the RX is moved toward left or right to implement various coupling ratios. Fig. 9(c) provides the coupling coefficients for various k_2/k_1 ratios for different vertical separation between TX and RX, which are used throughout the experiments.

For all experiments with different positions/separations, the received voltage is regulated to be 15 V by manually adjusting the inverter input. The simulated and measured efficiencies include dc-to-ac inverter efficiency, coil-to-coil efficiency, and rectifier efficiency. The simulation is done using LTspice software.

Fig. 10 compares the efficiencies of 2-TX and 1-TX system in order to verify the discussions in Section II. For 2-TX mode, the coil currents of each TX are set to be identical to each other. For 1-TX mode, the TX#2 is deactivated by setting the coil current of TX#2 to zero. For the relative coupling k_2/k_1 of $\sim$0, the receiver is initially located at right edge of Fig. 9(b). To increase the relative coupling k_2/k_1, the RX is moved gradually from right to left. The RX sweep stops at $k_2/k_1 = 1$, where the RX is located at the midpoint between TX#1 and TX#2.

From Fig. 10, it can be seen that the efficiencies of 2-TX and 1-TX systems intersect at k_2/k_1 ratio of $\sim$0.41 for different vertical separations and load currents. For k_2/k_1 ratio higher than 0.41, which corresponds to the RX location near midpoint, 2-TX case achieves higher efficiency. However, for k_2/k_1 ratio below 0.4 which means the RX is far from TX#2, the TX#2 should be turned-OFF for higher efficiency. The simulated inverter efficiency of Fig. 10(d) shows that the inverter efficiency is relatively constant compared to the large variations of overall system efficiency. The rectifier efficiency is the same because the rectifier output is always regulated to 15 V. Therefore, most of the efficiency variations are due to the coil-to-coil efficiency that is analyzed in Section II.

Figs. 11 and 12 present the efficiency when the respective coil currents of each TX are adjustable as in Section III, in contrast to the fixed identical coil currents of Section II. The TX coil currents I_{TX1} and I_{TX2} are adjusted by manually changing the input dc voltage of each inverter. During the current ratio adjustment, the dc output voltage of receiver is maintained to be 15 V by manually adjusting the TX inverter inputs.

For Fig. 11(a), the receiver location is fixed at Fig. 9(b) so that the k_2/k_1 ratio is 0.61. It shows that the maximum efficiency occurs when the TX current ratio $I_{\mathrm{TX2}}/I_{\mathrm{TX1}}$ is also at 0.61 which is the same with coupling ratio. In Fig. 11(b), the receiver location and therefore the k_2/k_1 ratio are changed to 0.4. As a result, the maximum efficiency occurs when the TX coil current ratio is at 0.4. These results are derived and expected in Section III. The same phenomenon is observed at different vertical separations of 5.8 cm in Fig. 12.

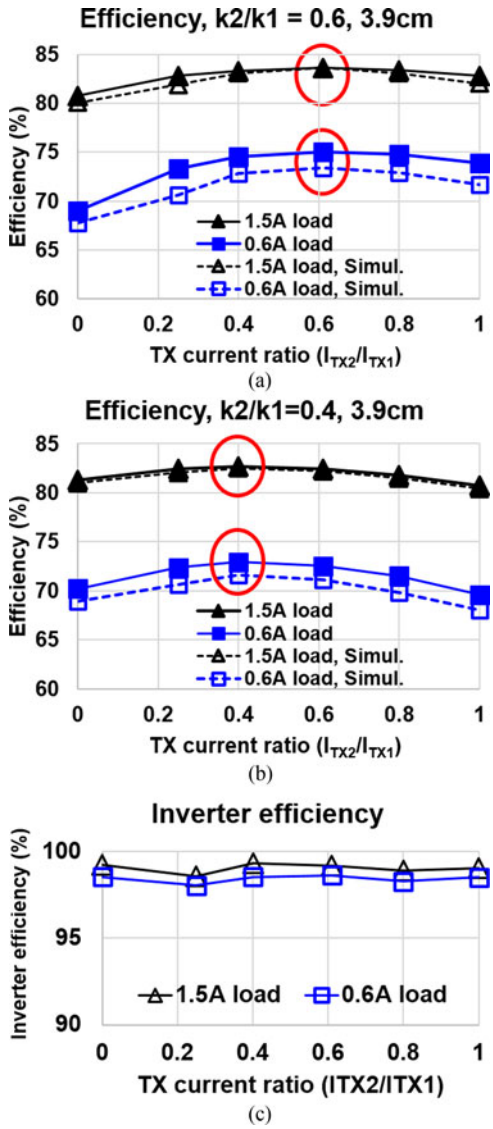

Fig. 11. Efficiencies when the relative ratio of TX coil currents is adjustable. The vertical separation between TX and RX is 3.9 cm. (a) The k_2/k_1 ratio is fixed to 0.6. The optimal current ratio occurs also at 0.6. (b) The k_2/k_1 ratio is set to 0.4. Similarly, the optimal TX current ratio is at 0.4. (c) Simulated inverter efficiency for $k_2/k_1 = 0.6$, which is relatively constant compared to overall system efficiency.

Fig. 13(a) shows the waveforms when only TX#1 is activated. This is a typical normal waveform of the LCC inverter. However, once TX#2 also starts operation as in Fig. 13(b), the TX#1 is deviated from resonance matching because its effective L_{TX} is increased due to the nonzero I_{TX2} term of (16). This off-tuning can be compensated by reducing the capacitor value of C_S such that (17-b) is satisfied. The compensated result is shown in Fig. 13(c).

A. Discussion

Although turning the weaker TX OFF would limit the maximum power capability, the planar array of TX coil should be

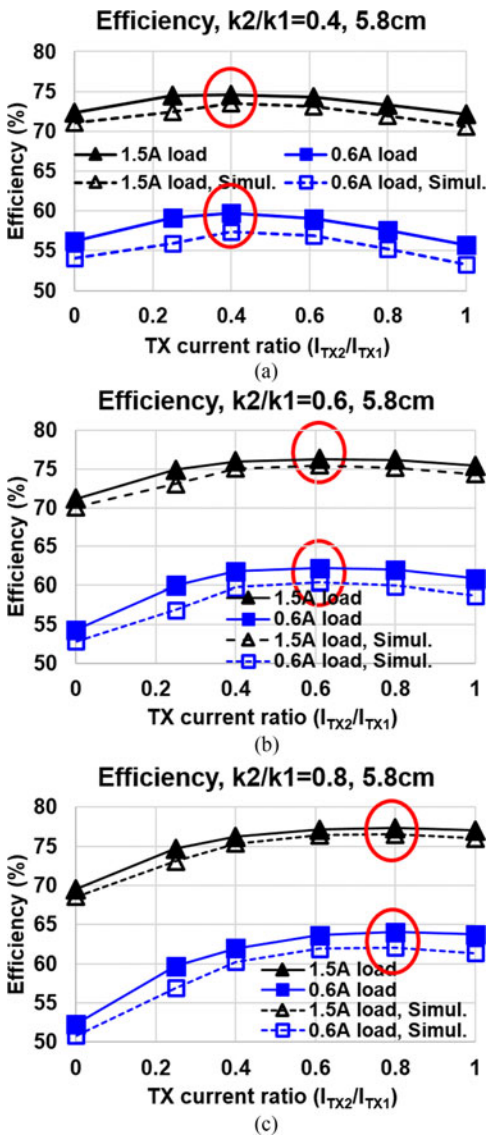

Fig. 12. Efficiencies when the relative ratio of TX coil currents is adjustable. The vertical separation is 5.8 cm. The k_2/k_1 ratios are set to (a) 0.4, (b) 0.6, and (c) 0.8, respectively.

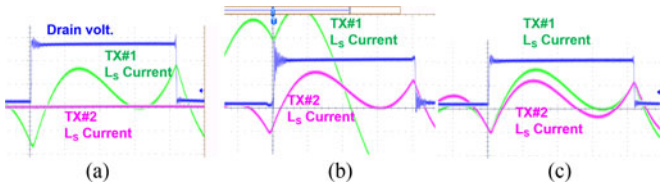

Fig. 13. Waveforms for the LCC resonant inverter. (a) Normal waveforms when only TX#1 is activated and TX#2 is OFF. (b) TX#2 is also activated with $I_{\mathrm{TX1}} = I_{\mathrm{TX2}}$. Due to the coupling between TX#1 and TX#2, the effective inductance of TX#1 is increased, resulting in the resonance mismatching. (c) Corrected to normal waveforms by reducing the C_S value.

designed such that 1-TX operation can also satisfy the power requirement of RX. Looking at Fig. 9(b), the worst-case scenario is when the receiver position is at right-edge location. The TX array should still be able to deliver the required power regardless of RX location. In worst-case location, TX#2 contributes negligible power and, therefore, the required power should solely be supplied by TX#1. Therefore, to cope with the worst-case location, a single TX should have the capability of delivering sufficient power and, hence, there is no need to activate both TXs for the purpose of maximum power. Now that 1-TX is able to satisfy the required power, it is better to achieve higher efficiency by turning the weaker TX OFF.

Although the fabrication cost will be increased due to additional inverters and tuning circuits, simply driving all the TX coils using a single inverter will lead to efficiency degradation if there are uncoupled TX coils. As can be seen from Fig. 10, driving both TXs reduces the efficiency by $\sim$10% if one TX is not coupled to RX. Note that high efficiency is essential to apply for governmental certification marks such as EnergyStar [27]. Such specifications require power conversion efficiency higher than certain level. Therefore, increasing the efficiency is a major concern for product certification, especially for wireless power products because of their typical low efficiency.

The size and weight problem of additional inverters would not be significant because the arrayed TX configuration targets wide charging area. In fact, the necessity of multiple TXs is due to the wide coverage area. The additional inverters may not be the areal burden because the system area and volume are also large to accommodate wide charging area. Regarding the weight, the TX array station is to be embedded underneath the surface or to be mounted on top of a surface. Therefore, the weight increment may not be an issue.

VI. Conclusion

The optimal driving of 2-TX system is investigated to maximize the power transfer efficiency of magnetic wireless power transfer. To account for more general usage scenarios, the couplings between each TX to an RX are assumed to be different. Two cases are studied. For simple low-cost applications, the TX coil currents are fixed to be identical. Second case is more sophisticated application where the relative magnitude of each TX coil current is allowed to be adjusted.

Theoretical and experiment results indicate that the coil current ratio should be set to the coupling coefficient ratio in order to obtain the highest efficiency. This achieves higher efficiency than the 1-TX operation and the same-current-2-TX operation. However, for applications where low-cost and simple implementation are important, the TX current adjustment may not be allowed. For such low-cost system, the TX coil currents are usually set to be identical. Then, a specific TX should be turned OFF and 1-TX operation is more efficient *as long as* the weak coupling is less than 0.41 times of stronger coupling (or, 2-TX is more efficient if the weaker coupling is higher than 0.41 times of stronger coupling). Note that the results are not verified for three or more TXs, and it would be one of the further research topics.

The results are simple but universal in that they relate the coil current ratio with the coupling coefficient ratio—the results are independent of the TX-to-RX separation and the load variations. They provide guideline for the optimal selection of TX element(s) and coil currents among the arrayed TXs for the highest overall efficiency.

APPENDIX

A. Inverter Loss and the Number of Inverters

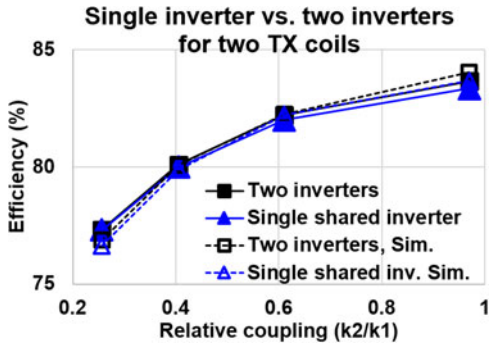

Fig. A1. Two-inverter two-coil system is compared with the single-inverter two-coil system. The power loss from gate driving circuits is accounted for. Increasing the number of inverter does not exacerbate the losses from inverter.

TABLE A-I
LOSS BREAKDOWN OF FIG. A1

Losses	One inverter (W)	Two inverters (W)
TX coil	2.53	2.54
RX coil	0.42	0.42
Rectifier	1.24	1.24
Inverter switch	0.504	0.368
Gate drive	0.025	0.05
RX load	24.23	24.29

The two-inverter two-coil system is compared with the single-inverter two-coil system. For the latter case, the two coils share one inverter. The input and RX output voltage characteristics of both cases are measured to be the same except for a small efficiency difference. The overall system efficiency of the two-inverter two-coil system is slightly higher than that of the one-inverter two-coil system. Therefore, *increasing the number of inverters does not exacerbate the losses from inverter*. This result is expected because the dc input current is divided into two inverters for the given RX output power. The current flowing through the switches and tuning inductor is reduced per one path, reducing the conduction and switching losses per one path. Recall that the conduction loss is proportional to I^2R where I and I^2R are reduced to half and 1/4, respectively. However, the improvement in overall efficiency is less than 1% and this is not the main claim of this paper. Rather, the key point of this section is that increasing the number of inverters does not at least exacerbate the losses of inverters.

B. In-Phase Coil Current by the LCC Inverter

The KVL equations for inverter-TX #1 of Fig. A2 are

$$\mathbf{V_{in1}} = j\omega L_S \mathbf{I_{in1}} + \left(j\omega L_{\mathrm{TX}} + \frac{1}{j\omega C_S}\right)\mathbf{I_{TX1}} + j\omega k_{\mathrm{TX}} L_{\mathrm{TX}} \mathbf{I_{TX2}} + j\omega k_1 \sqrt{L_{\mathrm{TX}} L_{\mathrm{RX}}}\,\mathbf{I_{RX}} \quad \text{(A1)}$$

$$\mathbf{V_{in1}} = j\omega L_S \mathbf{I_{in1}} + \frac{1}{j\omega C_P}\left(\mathbf{I_{in1}} - \mathbf{I_{TX1}}\right). \quad \text{(A2)}$$

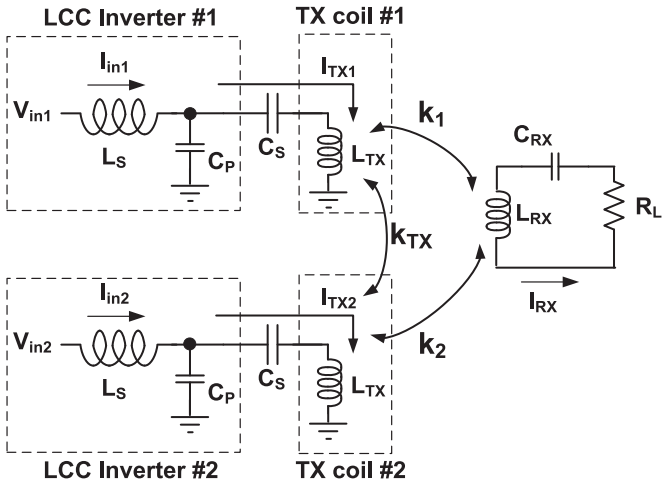

Fig. A2. Two LCC inverters and TX coils with different coupling factors of k_1 and k_2. The TX coil currents I_{TX1} and I_{TX2} are in-phase with each other regardless of k_1 and k_2.

Note that it is (A1), not (A2), that is affected by couplings k_1, k_2, and k_{TX}. Equation (A2) is independent of couplings. Equation (A2) can be rearranged to

$$\mathbf{V_{in1}} = \left(j\omega L_S + \frac{1}{j\omega C_P}\right)\mathbf{I_{in1}} - \frac{1}{j\omega C_P}\mathbf{I_{TX1}}. \quad \text{(A2-a)}$$

One of the design relation of the LCC inverter is $\frac{1}{\sqrt{L_S C_P}} = \omega$ [19]. Substituting this relation into (A2-a) cancels the term in parenthesis. This gives $\mathbf{V_{in1}} = -\frac{1}{j\omega C_P}\mathbf{I_{TX1}}$. In other words

$$\mathbf{I_{TX1}} = -j\omega C_P \mathbf{V_{in1}}. \quad \text{(A2-b)}$$

Equation (A2-b) states that I_{TX1} is 90 degree slower than V_{in1} regardless of couplings.

Following the same procedure, the TX coil #2 current is obtained as

$$\mathbf{I_{TX2}} = -j\omega C_P \mathbf{V_{in2}}. \quad \text{(A2-c)}$$

I_{TX2} is also 90 degree slower than V_{in2} regardless of couplings. Therefore, as long as the input voltage V_{in1} and V_{in2} are in-phase by the shared clocks, the coil currents I_{TX1} and I_{TX2} have the same phase to each other regardless of different couplings. Note that the same derivation can be found in [19].

REFERENCES

[1] J. Casanova, Z. Low, J. Lin, and R. Tseng, "Transmitting coil achieving uniform magnetic field distribution for planar wireless power transfer system," in *Proc. Radio Wireless Symp.*, 2009, pp. 530–533.
[2] L. Shen, W. Tang, H. Xiang, and W. Zhuang, "Uniform magnetic field of the planar coil with new winding structure for displacement-insensitive WPT," in *Proc. Commun. Probl.-Solving*, 2014, pp. 394–396.
[3] J. Kim, D.-H. Kim, and Y.-J. Park, "Free-positioning wireless power transfer to multiple devices using a planar transmitting coil and switchable impedance matching network," *IEEE Trans. Microw. Theory Techn.*, vol. 64, no. 11, pp. 3714–3722, Nov. 2016.
[4] S. Mirbozorgi, H. Bahrami, M. Sawan, and B. Gosselin, "A smart multicoil inductively coupled array for wireless power transmission," *IEEE Trans. Ind. Electron.*, vol. 61, no. 11, pp. 6061–6070, Nov. 2014.
[5] X. Shi and J. Smith, "Large area wireless power via a planar array of coupled resonators," in *Proc. IEEE Int. Workshop Antenna Technol.*, 2016, pp. 200–203.

[6] F. Jolani, Y.-Q. Yu, and Z. Chen, "A planar magnetically-coupled resonant wireless power transfer using array of resonators for efficiency enhancement," in *Proc. IEEE Int. Microw. Symp.*, 2015, pp. 1–4.
[7] W. Zhong, X. Liu, and S. Hui, "A novel single-layer winding array and receiver coil structure for contactless battery charging systems with free-positioning and localized charging features," *IEEE Trans. Ind. Electron.*, vol. 58, no. 9, pp. 4136–4144, Sep. 2011.
[8] S. Hui, "Planar wireless charging technology for portable electronic products and Qi," *Proc. IEEE*, vol. 101, no. 6, pp. 1290–1301, Jun. 2013.
[9] X. Liu and S. Hui, "Simulation study and experimental verification of a universal contactless battery charging platform with localized charging features," *IEEE Trans. Power Electron.*, vol. 22, no. 6, pp. 2202–2210, Nov. 2007.
[10] R. Johari, J. Krogmeier, and D. Love, "Analysis and practical considerations in implementing multiple transmitters for wireless power transfer via coupled magnetic resonance," *IEEE Trans. Ind. Electron.*, vol. 61, no. 4, pp. 1774–1783, Apr. 2014.
[11] I.-J. Yoon and H. Ling, "Investigation of near-field wireless power transfer under multiple transmitters," *IEEE Antennas Wireless Propag. Lett.*, vol. 10, pp. 662–665, Jun. 2011.
[12] D. Ahn and S. Hong, "Effect of coupling between multiple transmitters or multiple receivers on wireless power transfer," *IEEE Trans. Ind. Electron.*, vol. 60, no. 7, pp. 2602–2613, Jul. 2013.
[13] B. Choi, J. Kim, J. Cheon, and C. Rim, "Synthesized magnetic field focusing using a current-controlled coil array," *IEEE Magn. Lett.*, vol. 7, Feb. 2016, Art. no. 6501504.
[14] P. Kong and H. Ku, "Efficiency optimizing scheme for wireless power transfer system with two transmitters," *Electron. Lett.*, vol. 52, no. 4, pp. 310–312, Feb. 2016.
[15] S. Hui and W. Ho, "A new generation of universal contactless battery charging platform for portable consumer electronic equipment," *IEEE Trans. Power Electron.*, vol. 20, no. 3, pp. 620–627, May 2005.
[16] B. Lee, D. Ahn, and M. Ghovanloo, "Three-phase time-multiplexed planar power transmission to distributed implants," *IEEE J. Emerging Sel. Topics Power Electron.*, vol. 4, no. 1, pp. 263–272, Mar. 2016.
[17] S. Zhou and C. Chris Mi, "Multi-paralleled LCC reactive power compensation networks and its tuning method for electric vehicle dynamic wireless charging," *IEEE Trans. Ind. Electron.*, vol. 63, no. 10, pp. 6546–6556, Oct. 2016.
[18] M. Kissin, C.-Y. Huang, G. A. Covic, and J. T. Boys, "Detection of the tuned point of a fixed-frequency LCL resonant power supply," *IEEE Trans. Power Electron.*, vol. 24, no. 4, pp. 1140–1143, Apr. 2009.
[19] Z. Pantic, S. Bai, and S. Lukic, "ZCS LCC-compensated resonant inverter for inductive-power-transfer application," *IEEE Trans. Ind. Electron.*, vol. 58, no. 8, pp. 3500–3510, Aug. 2011.
[20] D. Ahn and S. Hong, "Wireless power transfer resonance coupling amplification by load-modulation switching controller," *IEEE Trans. Ind. Electron.*, vol. 62, no. 2, pp. 898–909, Feb. 2015.
[21] D. Ahn, S. Kim, J. Moon, and I.-K. Cho, "Wireless power transfer with automatic feedback control of load resistance transformation," *IEEE Trans. Power Electron.*, vol. 31, no. 11, pp. 7876–7886, Nov. 2016.
[22] Y. Sohn, B. H. Choi, E. S. Lee, G. C. Lim, G.-H. Cho, and C. T. Rim, "General unified analyses of two-capacitor inductive power transfer systems: Equivalence of current-source SS and SP compensations," *IEEE Trans. Power Electron.*, vol. 30, no. 11, pp. 6030–6043, Nov. 2015.
[23] E. Waffenschmidt, "Dynamic resonant matching method for a wireless power transmission receiver," *IEEE Trans. Power Electron.*, vol. 30, no. 11, pp. 6070–6077, Nov. 2015.
[24] Y. Lim, H. Tang, S. Lim, and J. Park, "An adaptive impedance-matching network based on a novel capacitor matrix for wireless power transfer," *IEEE Trans. Power Electron.*, vol. 29, no. 8, pp. 4403–4413, Aug. 2014.
[25] Y. Li, R. Mai, Y. Liu, and Z. He, "Efficiency optimising strategy for dual-coupled transmitters based WPT systems," *Electron. Lett.*, vol. 52, no. 22, pp. 1877–1879, Oct. 2016.
[26] S. Liu, M. Liu, S. Yang, C. Ma, and X. Zhu, "A novel design methodology for high-efficiency current-mode and voltage-mode class-E power amplifiers in wireless power transfer systems," *IEEE Trans. Power Electron.*, vol. 32, no. 6, pp. 4514–4523, Jun. 2017.
[27] ENERGY STAR Program Requirements for Computers Partner Commitments, Mar. 2016. [Online]. Available: www.energystar.gov.
[28] "The Qi Wireless Power Transfer System, Power Class 0 Specification, Parts 4: Reference Designs," Wireless Power Consortium, Apr. 2016.
[29] S. Y. R. Hui and W. C. Ho, "A new generation of universal contactless battery charging platform for portable consumer electronic equipment," *IEEE Trans. Power Electron.*, vol. 20, no. 5, pp. 620–627, May 2005.
[30] U.-M. Jow, M. Kiani, X. Huo, and M. Ghovanloo, "Towards a smart experimental arena for long-term electrophysiology experiments," *IEEE Trans. Biomed. Circuits Syst.*, vol. 6, no. 5, pp. 414–423, Oct. 2012.

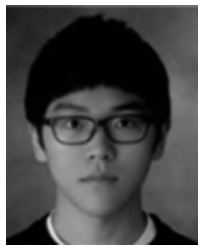

Sungryul Huh is currently working toward the B.S. degree in electrical engineering at Incheon National University, Incheon, South Korea.

He worked in a part-time research position during his B.S. study in electrical engineering. His research interest focuses on wireless power electronics circuit.

Dukju Ahn received the B.S. degree from Seoul National University, Seoul, South Korea, in 2007, and the M.S. and Ph.D. degrees from the Korea Advanced Institute of Science and Technology, Daejeon, South Korea, in 2010 and 2012, respectively, all in electrical engineering.

He is currently with Incheon National University, Incheon, South Korea. His research interests include wireless power transfer, power conversion, and analog/RF integrated circuit design for biomedical and portable applications.